HHS Public Access

Author manuscript

Neuroscience. Author manuscript; available in PMC 2017 May 13.

Published in final edited form as:

Neuroscience. 2016 May 13; 322: 370–376. doi:10.1016/j.neuroscience.2016.02.059.

MECHANISMS UNDERLYING THE FORMATION OF THE AMYGDALAR FEAR MEMORY TRACE: A COMPUTATIONAL PERSPECTIVE

Feng Feng[1], **Pranit Samarth**[1], **Denis Paré**[2], and **Satish S. Nair**[1]

[1]Department of Electrical and Computer Engineering, University of Missouri, Columbia, MO

[2]Center for Molecular and Behavioral Neuroscience, Rutgers, The State University of New Jersey, Newark, NJ, USA

Abstract

Recent experimental and modeling studies on the lateral amygdala (LA) have implicated intrinsic excitability and competitive synaptic interactions among principal neurons (PNs) in the formation of auditory fear memories. The present modeling studies, conducted over an expanded range of intrinsic excitability in the network, revealed that only excitable PNs that received tone inputs participate in the competition. Strikingly, the number of model PNs integrated into the fear memory trace remained constant despite the much larger range considered, and model runs highlighted several conditioning-induced tone responsive characteristics of the various PN populations. Furthermore, these studies showed that although excitation was important, disynaptic inhibition among PNs is the dominant mechanism that keeps the number of plastic PNs stable despite large variations in the network's excitability. Finally, we found that the overall level of inhibition in the model network determines the number of projection cells integrated into the fear memory trace.

Graphical abstract

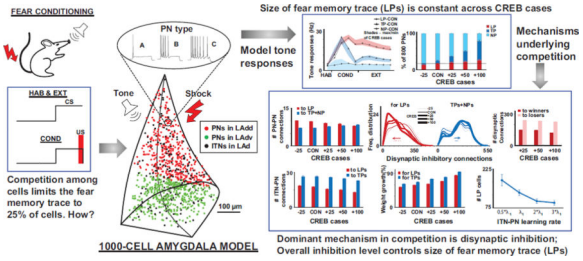

Correspondence may be sent to: Satish S. Nair, Professor, Electrical and Computer Engineering, University of Missouri, Columbia, MO, 65211, Tel: 573-882-2964; Fax: 573-882-0397 nairs@missouri.edu.

Keywords

biophysical model; sparse coding; Hebbian learning

INTRODUCTION

Animals are predisposed to learn fear by experience. Indeed, they learn to fear new stimuli quickly and robustly in a classical fear conditioning paradigm where a neutral sensory stimulus (such as tone; conditioned stimulus, CS) acquires the ability to elicit fear responses after a few pairings with a noxious stimulus (such as foot shock; unconditioned stimulus, US). The lateral amygdala (LA) is a critical site of plasticity for the storage of auditory Pavlovian fear memories in rodents (LeDoux, 2000; Pape and Pare, 2010). Repa et al. (2001) showed that ~25% of principal LA neurons (PNs) acquire conditioning induced plasticity, and these were of two types: transiently plastic (TP) neurons that display increases in CS responsiveness that last for only a few trials, and long-term plastic (LP) neurons whose CS responses are persistently increased, even resisting extinction training (Repa et al., 2001). Neurons that do not fall into the TP or LP categories are designated in the following as non-plastic (NP). Interestingly, a recent study showed that only 25% of PNs store this 'fear memory trace' (Han et al., 2007) although 70% receive CS and US inputs (Quirk et al., 1995; Repa et al., 2001; Rumpel, et al. 2005).

Computational models of fear learning have typically used connectionist or firing rate formalisms in the past, and have provided valuable insights (Armony et al., 1997; Krasne et al., 2011; Moren and Balkenius, 2000; Moustafa et al., 2013; Vlachos et al., 2011). However, they have not been able to incorporate emerging data about cellular, synaptic and neuromodulatory mechanisms involved in fear. Our recent biophysical network model of LA (Kim et al., 2013a) was the first to incorporate such neurophysiology data into biophysical models of the fear circuit, and it successfully replicated the findings of Repa et al. (2001).

Prior work has established that the incidence of PNs expressing activated CREB is high among plastic cells (Han et al., 2007; Han et al., 2009). The fact that CREB increases intrinsic neuronal excitability (Zhou et al., 2009), led Han et al. (2007) to suggest that the fear memory trace preferentially recruits PNs with higher intrinsic excitability. However, these authors also found that increasing the number of CREB-expressing cells did not augment the number of plastic cells (Han et al., 2007). Consistent with these results, in another recent study (Kim et al., 2013b), we found that highly excitable PNs were preferentially recruited as plastic cells, a prediction that was later validated experimentally (Yiu et al., 2014). Furthermore, although CREB-overexpression led to the addition of new model plastic cells (hereafter termed "winner cells"), many originally plastic neurons dropped out from the plastic category ("loser cells"), resulting in a stable number of plastic cells. Analysis of the connections formed by winner and loser cells (see cartoon in Fig. 1A) provided support for the notion that competitive synaptic mechanisms limit the number of PNs storing fear memories. For instance, the PNs that increased their firing rates after conditioning or plastic PNs (red triangles in Fig. 1A) were found to receive fewer disynaptic

inhibitory connections from other plastic PNs via interneurons, compared to non-plastic PNs (blue triangles). Solid lines between cells indicate training induced changes in connections, while dotted lines indicate unchanged connections. Also, interneurons (grey filled circles) that received relatively larger numbers of excitatory connections (red connections) from plastic PNs were found to be more effective at inhibiting PNs (via black connections) making them non-plastic (NP, blue). Many of the factors that regulate this competition were left unexplored in our previous study (Kim et al., 2013b). Here, we consider a wider range of competitive scenarios which revealed important insights including the composition of PNs that participated in the memory trace, the formation of the different tone-responsive populations, and the roles of banding among PNs and of neuromodulation in the competitive process. The study also conclusively highlighted inhibition as the key mechanism in the competition, and showed that the overall level of inhibition in the system controlled the size of the memory trace.

EXPERIMENTAL PROCEDURES

The present study used the 1000-cell biophysical model of the dorsal part of LA (LAd) we reported recently (Kim et al., 2013a, 2015). The salient aspects of the model are provided below.

Single cell and network models

We used a Hodgkin-Huxley formulation to develop single cell models. The model PNs had three compartments, and reproduced the active and passive membrane properties, including the diversity of spike frequency adaptation seen in LA (Faber et al., 2001; Sah et al., 2003) comprising three types of regular spiking PNs, with high (type-A), intermediate (type-B), or low (type-C) spike frequency adaptation (Fig. 1B; matched data in Faber et al. 2001), due to the differential expression of a Ca^{2+}-dependent K^+ current (highest in type-A and lowest in type-C). LA also contains local GABAergic interneurons that exhibit various firing patterns, even among neurochemically-homogeneous subgroups (Pape and Paré, 2010). However, the majority displays a fast-spiking pattern, whose membrane properties were reproduced in our 2-compartment ITN model.

LAd is estimated to have 24,000 principal cells in LAd (Tuunanen and Pitkanen, 2000). We developed a scaled down (30:1) version of LAd that included 800 principal cells. Because the proportion of interneurons to principal cells is 20:80, the model included 200 interneurons. Principal cells and interneurons were distributed randomly in a realistic tri-dimensional representation of the horn-shaped LAd (Kim et al., 2015). Connectivity among as well as between PNs and ITNs was based on prior experiments on the intrinsic LA network (Samson and Pare, 2006). It should be noted that in our model, CREB (or intrinsic excitability) did not determine the initial connectivity of the cells. Instead, independently of whether particular principal cells were Type-A, B, or C, we set up probabilistic gradients of connectivity based on earlier physiological studies of the intrinsic LA network.

Synaptic plasticity

Model synapses could undergo activity-dependent synaptic plasticity, consistent with the experimental literature. All AMPA (except for those delivering shock or background inputs) and GABA synapses in the model were endowed with long-term postsynaptic plasticity (Bauer and LeDoux, 2004; Kim et al., 2013a). This form of plasticity was implemented using a learning rule that uses the concentration of a post-synaptic calcium pool at each modifiable synapse (Shouval et al., 2002). Calcium entered post-synaptic pools at excitatory synapses via NMDA receptors (and AMPA receptors for interneurons) and voltage-gated calcium channels (VGCCs). Similarly, calcium for pools at inhibitory synapses came from post-synaptic intra-cellular stores and VGCCs (Li et al, 2009). All model AMPA and GABA synapses also exhibited short-term presynaptic plasticity, with short-term depression at interneuron to principal cell and principal cell to interneuron connections (Woodruff and Sah, 2007). The model also incorporated the effects of dopamine and norepinephrine on LAd cells, based on prior experimental reports, as detailed in Kim et al. (2013a).

Neuromodulator effects

Neuromodulators have long been implicated in fear and anxiety, and are known to regulate Pavlovian fear learning and synaptic plasticity in LA (Bissière et al., 2003; Tully et al., 2007). Conditioned aversive stimuli alter the activity of ventral tegmental area (Feenstra et al., 2001) and locus coeruleus neurons (Guarraci and Kapp, 1999), which in turn modulate fear and anxiety through their widespread forebrain projections, including to the amygdala. Therefore, the model incorporated the effects of dopamine (DA) and norepinephrine (NE) on LAd cells, based on prior experimental reports, as detailed in Kim et al., 2013a.

Inputs and conditioning protocol

To reproduce the low spontaneous firing rates of PNs in baseline conditions (Gaudreau and Pare, 1996), Poisson-distributed, random excitatory background inputs were delivered to all model cells, resulting in average spontaneous firing rates of 0.7 Hz for PNs and 5.5 Hz for ITNs. The CS and US inputs were represented by glutamatergic synapses acting via AMPA and NMDA receptors. The frequency of thalamic and cortical tone inputs during habituation was set to 20 Hz. The following distribution of inputs was used for the simulations: uniform total tone density throughout LAd with 70% of the dorsal aspect of LAd (LAdd) cells receiving thalamic and 35% receiving cortical tone projections, and the opposite for the ventral aspect of LAd (LAdv), i.e., 35% of LAdv cells receiving thalamic and 70% receiving cortical tone projections. The shock inputs were distributed uniformly to 70% of LAd cells. The schedule of tone and shock inputs in the simulations was based on in vivo studies (Quirk et al., 1995).

The auditory fear conditioning protocol (Fig. 1C) included three phases (habituation, conditioning and recall), comprised of 8, 16 and 4 trials, respectively. Each trial featured a 0.5 sec tone CS followed by a 3.5 sec gap. Only during conditioning, a shock (100 Hz) was administered 100 msec prior to the end of the tone, so that they co-terminated. The frequency of thalamic and cortical tone inputs was increased to 40 Hz after the first and sixth conditioning trials, respectively (Bordi and LeDoux, 1994; Quirk et al., 1995; Maren et al., 2001). Although we used the same model as in Kim et al. (2013a), a more stringent

criterion was used to classify the output tone responses: a minimum z-score of 5.5 and a threshold of 10 Hz was used to define TP and LP cells; if the average z-score of the last two conditioning blocks was less than 75% of the same value for the first two blocks, it was classified as TP, else as LP.

As cited, the LAd network was set up using probabilistic gradients for intrinsic gradients (ranging from 2% to 23%; Samson and Pare, 2006). We performed five different instantiations of these gradients as well as the extrinsic (tone and shock) connections and synaptic delays. Unless stated otherwise, all results represent averages ± SEM across these five runs, performed using parallel NEURON (Carnevale and Hines, 2006) running on a Beowulf supercluster with a time step of 10 μs. The primary model used in this study is available on the ModelDB public database (http://senselab.med.yale.edu/ModelDB/) as part of our previous publication (Kim et al., 2013a).

RESULTS

To analyze competitive synaptic interactions among LA neurons, we simulated the CREB overexpression ($CREB^+$) or downregulation ($CREB^-$) experiments of Han and colleagues by converting a randomly selected subset of type-A neurons to type-C (from 25% to 100%; denoted as $CREB^+$25%, $CREB^+$50% and $CREB^+$100%), and type-B-C neurons to type-A (25%; $CREB^-$ 25%), without changing other model parameters. We then examined how these changes altered the impact of conditioning on the CS responsiveness of PNs. These analyses resulted in several novel insights related to the formation of the fear memory trace.

Although our previous study showed that more excitable model cells (types B and C) were preferentially recruited into the trace, the underlying mechanism were not mapped out in detail. Expansion of the CREB range from 25% to 100% helped explore the underlying mechanisms in a more comprehensive manner. A key finding from the present study was that a smaller subset of PNs than reported previously participated in the competition. This in turn helped identify synaptic interactions underlying competition more sharply and highlighted disynaptic inhibition as the salient mechanism that endowed the network with the ability to be highly discriminative in its recruitment of PNs into the memory trace (LPs). These findings are described below in sequence.

First, despite the large increase or decrease in the numbers of excitable type B and C neurons produced in the $CREB^+$ or $CREB^-$ simulations, the tone responses of LP, TP and non-plastic cells remained within biological ranges (Quirk et al. 1995,1997; Repa et al., 2001), even for the extreme competition cases of $CREB^+$50% and $CREB^+$100% (Fig. 2A). Importantly, the number of model LP but not TP cells remained approximately constant across the CREB cases (Fig. 2B). An analysis of cellular excitability, and network connectivity, helped identify the subset of PNs that participated in the competition, and how they did so. Specifically, (i) Across all CREB cases, LPs consisted only of high intrinsically excitable type B and C PNs, and none of type A, as previously reported (Kim et al., 2013b). However, a new finding was that within this group of type B and C PNs (e.g., total 400 for control), only those that received both tone and shock (n=225, control), or only tone (n=95, control) inputs participated in the competition (because the tone synapses to these cells grew

faster causing these cells to fire more than the PNs that did not receive tone), the 'competition group' (Fig 2C). Indeed, in the control and extreme CREB^{+}100% cases, respectively, 98 and 99% of LPs had this property. Hence, in subsequent analyses, we will only consider PNs that receive tone or tone and shock inputs (Fig. 3 A–C). (ii) Within the competition group (typical composition shown in Fig. 2C), LPs tended to receive significantly more excitatory inputs (Fig. 3A) from other PNs than TP and NP cells for all the cases except the CREB^{+}100% condition. More importantly, LPs in the competition group received markedly less disynaptic inhibition from other competing PNs than TP and NP cells for all the cases (excitation: two way ANOVAs, $F=126.1$, $DF=1$, $p<0.0001$; disynaptic inhibition: two way ANOVAs, $F=774.6$, $DF=1$, $p<0.0001$), causing the LPs to fire more compared to the others. Increasing levels of competition (CREB - 25% to CREB^{+}100%) highlighted an interesting mechanism supporting the competition. As competition increased, the network selected PNs that received the fewest disynaptic inhibitory connections from other PNs in the competition group. In the frequency distributions of the number of disynaptic inhibitory inputs (Fig. 3B), this is evidenced by the progressive shift of the distributions to the left for LPs (Fig. 3B1) and to the right of TPs and NPs (Fig. 3B2). (iii) We then considered the subgroups of winner and loser LPs, and calculated the excitation and disynaptic inhibition they received from other PNs in the competition group. The number of disynaptic inhibitory inputs from other PNs onto loser LPs, compared to those onto winner LPs, continued to be significantly higher (Fig. 3C; two way ANOVAs, $F=529.9$, $DF=1$, $p<0.0001$). Yet, the number of excitatory inputs to loser LPs was higher (10.3 ± 0.2), compared to those onto winner LPs (8.1 ± 0.1; not shown; two way ANOVAs, $F=128.9$, $DF=1$, $p<0.0001$), again indicating that disynaptic inhibition is the dominant factor supporting the competition.

Second, several model behaviors supported the notion that plastic PNs banded together in the competition to inhibit potentiation of plasticity in other cells: (i) conditioning induced growth in PN-PN weights for LP-LP connections was significantly higher ($70.2 \pm 0.4\%$), compared to such connections between NPs ($15.9 \pm 0.4\%$; two way ANOVAs, $F=4998.0$, $DF=1$, $p<0.0001$); (ii) similarly, conditioning induced growth in tone-PN synaptic weights was significantly higher for plastic cells ($183.3 \pm 0.5\%$) compared to non-plastic cells ($81.3 \pm 1.5\%$; two way ANOVAs, $F=7149.3$, $DF=1$, $p<0.0001$); (iii) when all model PN-PN weights were set to zero for a typical run, the number of LP cells dropped by 70% in the control case (Chi-square test, $p<0.0001$), and the number of TP cells dropped to zero (Chi-square test, $p<0.0001$); (iv) finally, when plasticity was inactivated in only PN-PN connections, the number of LP cells decreased by 2% (Chisquare test, $p=0.77$), and TP cells by 29% (Chi-square test, $p=0.01$), suggesting that the PN-PN connections themselves may be more important for banding than the plasticity in these connections.

Third, TP cells are thought to be 'trigger' cells (Repa et al., 2001) although their role in fear learning is not understood. Our analysis provided insights into their potential function. Compared to LP cells, TP cells received considerably higher monosynaptic connections from ITNs across all CREB cases (Fig 3D; two way ANOVAs, $F=2297.7$, $DF=1$, $p<0.0001$). Also, compared to LP cells, TP cells exhibited significantly higher growth in ITN-PN connections (Fig 3E; two way ANOVAs, $F=4856.5$, $DF=1$, $p<0.0001$). The number of excitatory connections from plastic PNs to TP and LP cells was comparable, again

highlighting inhibition as a key factor in the formation of TP cells. This suggests that in the early stages of conditioning, plastic cells (TPs+LPs) band together and disynaptically inhibit potentiation of responses in non-plastic cells. However, later during conditioning, the tone responses of TP cells decrease due to significantly higher disynaptic inhibition (compared to LPs) from other plastic PNs. Consistent with this, the tone responses of TP cells decreased during the second half of conditioning, while those of LP cells did not (Fig. 2A). Although PN-PN weights between TP cells were high, training induced growth in the disynaptic inhibitory connections reduced the tone responses of TP cells to habituation levels by late conditioning. So, although excitation plays a role initially, inhibition is again the dominant mechanism in the formation of TP cells. More importantly, while these 'trigger' TP cells contribute to the formation of LP cells, they do not seem to play any role subsequently.

Fourth, although neuromodulation is known to play a role in the formation of fear memory traces (Bissière et al., 2003; Tully et al., 2007), the underlying mechanisms remain unclear. We performed inactivation experiments to address this question. When we inactivated DA and NE neuromodulator receptors during training almost half of the original trace, 42% (53/125) of LP and 63% (43/68) of TP cells, lost their tone-responsiveness, and became non-plastic cells. This suggests that neuromodulation is important for the formation of both types of tone-responsive cell populations. Interestingly, this inactivation led to a new competition among PNs, resulting in the memory trace stabilizing at 101 cells, of which 30 (30%) were from the originally non-plastic cell category. All remaining original TP cells (25/68) were converted to LP cells, while most of the remaining LP cells (71/125) 'survived' as LP cells. In an overall sense, blockade of neuromodulation resulted in a drop of LP cell numbers by 19% (Chi-square test, $p=0.02$) and a drop in their tone responses by 25% (t-test, $p<0.0001$); more dramatically, there was a 99% drop in TP cell numbers, virtually wiping them out (Chi-square test, $p<0.0001$). As cited above, inhibition plays a critical role in the formation of TP, but not LP, cells. Neuromodulators affected both excitation and inhibition of PNs (see Kim et al., 2013a for implementation). DA increases the GABA conductance during high neuromodulation state (Loretan, 2004). Also NE was shown to decrease NMDA conductance during late conditioning (Johnson et al., 2011). Inactivation of neuromodulators thus resulted in an effective decrease in inhibition and an increase in excitation during late conditioning, favoring LP but not TP cells. This explained why inactivation of neuromodulators virtually wiped out TP cells.

Lastly, we also investigated the hypothesis that the level of inhibition in the network constrained the size of the fear memory trace to 10–40% of PNs (Tovote et al., 2015). To test this, we varied both initial weights and learning rates of the three inhibitory pathways, ITN-PN, PN-ITN and tone- ITN, and found that the LP cell numbers changed proportionately, without appreciable changes in tone response magnitudes. A representative plot of the effect of changing the learning rate λ for the ITN-PN pathway on the number of plastic cells is shown in Fig. 3F, highlighting how the level of inhibition in the system controls the size of the fear memory trace.

DISCUSSION

Memories are sparsely encoded in cerebral networks. However, the neural substrates of such encoding are not well understood, including for amygdalar memories. The dorsal aspect of the lateral amygdala is an important site of plasticity during the formation of CS-US associations in auditory Pavlovian fear conditioning (LeDoux, 2000; Pape and Pare, 2010). This association is stored as a 'fear memory trace' involving about 25% of the PNs in LA (Han et al., 2007). The trace was hypothesized to result from a competitive process among PNs which restricted the size of the fear memory trace after CREB-induced increase in the number of excitable PNs (Han et al., 2007). Using our biophysical network model, we successfully replicated these findings (Kim et al., 2013b). An analysis of the model connections formed by winner and loser cells suggested that competitive synaptic mechanisms limit the number of PNs storing fear memories. However, many of the factors that regulate this competition were left unexplored, including the composition of the PNs recruited into the fear memory trace, the roles of the two classes of tone-responsive PNs and of neuromodulation during the coding, and the robustness of the findings.

Here we report important insights into the mechanisms underlying this competition that emerged when we extended the $CREB^{+}25\%$ case (as in experiments of Han et al. 2007 and our previous model) to $CREB^{+}100\%$ in steps of 25%. Remarkably, the tone responses of LP, TP and non-plastic cells (Fig. 2A) stayed within biological ranges (Quirk et al., 1995,1997; Repa et al., 2001) for even the extreme CREB manipulations, with a new observation that the number of model LP, but not TP cells remained approximately constant across the CREB cases (Fig. 2B). Furthermore, detailed analysis of the competition revealed that that only PNs that received extrinsic afferents of tone and shock, or only tone, participated in the competition. Within this competition group, additional analysis showed how PNs banded together to increase their firing rates and effectively inhibit other PNs. Importantly, disynaptic inhibition that a PN received from other PNs via ITNs was consistently seen to be the dominant mechanism implementing competition across all scenarios (Figs. 3A–C). Interestingly, this inhibitory mechanism was also key to the formation of TP cells, a group whose role has hitherto not been well understood. Although neuromodulation has been known to be important in memory formation, their role in encoding such memories is not clear. Model runs showed that neuromodulation was critical for memory formation, and highlighted the differential roles it had in the formation of LP and TP cell types. The model also helped shed light on two other poorly understood phenomena, the role of TP cells and factors that controlled the 'size' of the fear memory trace. Model runs showed that TP cells were important in the early stages of the memory storage but had no role once the memory was formed. Another key insight was that the level of inhibition in the system controlled the size of the fear memory trace (Fig. 3F).

CONCLUSIONS

In the amygdala, experimental studies have implicated cellular excitability and synaptic competition in the formation of auditory fear memories. In a prior modeling study, we confirmed that cellular excitability is a contributing factor. Here, we examined the synaptic mechanisms supporting the selective recruitment of the most excitable principal cells in the

memory trace. We found that only a particular group of highly excitable principal neurons compete: those with access to inputs about the conditioned stimulus. Of these, synaptic competition selects a subset and inhibition is the dominant mechanism that keeps their number relatively constant despite large variations in cellular excitability. Together with insights into several other underlying mechanisms, this study provides the first comprehensive account of the neural substrates of competition among PNs in fear memory formation. A challenge for future experiments will be to test these predictions using optogenetic tools to manipulate specific classes of neurons and their projections. The insights related to the underlying mechanisms of memory formation have potential applicability to sparse coding in other cerebral networks.

In addition, the finding that the level of intrinsic inhibition has such a profound influence on the integration of projection cells into fear memory traces has potential clinical relevance. Indeed, it implies that slight reductions in the amount of intrinsic inhibition could allow the number of PNs encoding fear memories to increase, compromising their stimulus specificity.

Acknowledgments

This research was supported in part by NIMH grants MH083710 to D.P. and MH087755 to S.S.N.

REFERENCES

Bauer EP, LeDoux JE. Heterosynaptic long-term potentiation of inhibitory interneurons in the lateral amygdala. J Neurosci. 2004; 24:9507–9512. [PubMed: 15509737]

Armony JL, Servan-Schreiber D, Romanski LM, Cohen JD, LeDoux JE. Stimulus generalization of fear responses: effects of auditory cortex lesions in a computational model and in rats. Cereb Cortex. 1997; 7:157–165. [PubMed: 9087823]

Bissière S, Humeau Y, Luthi A. Dopamine gates LTP induction in lateral amygdala by suppressing feedforward inhibition. Nat Neurosci. 2003; 6:587–592. [PubMed: 12740581]

Bordi F, LeDoux JE. Response properties of single units in areas of rat auditory thalamus that project to the amygdala. II. Exp Brain Res. 1994; 98:275–286. [PubMed: 8050513]

Carnevale, N.; Hines, M. The NEURON Book. UK: Cambridge University Press; 2006.

Faber ES, Callister RJ, Sah P. Morphological and electrophysiological properties of principal neurons in the rat lateral amygdala in vitro. J Neurophysiol. 2001; 85:714–723. [PubMed: 11160506]

Faber ES, Callister RJ, Sah P. Morphological and electrophysiological properties of principal neurons in the rat lateral amygdala in vitro. J Neurophysiol. 2001; 85:714–723. [PubMed: 11160506]

Feenstra MG, Vogel M, Botterblom MH, Joosten RN, de Bruin JP. Dopamine and noradrenaline efflux in the rat prefrontal cortex after classical aversive conditioning to an auditory cue. Eur J Neurosci. 2001; 13:1051–1054. [PubMed: 11264679]

Gaudreau H, Paré D. Projection neurons of the lateral amygdaloid nucleus are virtually silent throughout the sleep--waking cycle. J Neurophysiol. 1996; 75:1301–1305. [PubMed: 8867138]

Guarraci FA, Kapp BS. An electrophysiological characterization of ventral tegmental area dopaminergic neurons during differential Pavlovian fear conditioning in the awake rabbit. Behav Brain Res. 1999; 99:169–179. [PubMed: 10512583]

Han JH, Kushner SA, Yiu AP, Cole CJ, Matynia A, Brown RA, Neve RL, Guzowski JF, Silva AJ, Josselyn SA. Neuronal competition and selection during memory formation. Science. 2007; 316:457–460. [PubMed: 17446403]

Han JH, Kushner SA, Yiu AP, Hsiang HL, Buch T, Waisman A, Bontempi B, Neve RL, Frankland PW, Josselyn SA. Selective erasure of a fear memory. Science. 2009; 323:1492–1496. [PubMed: 19286560]

Hummos A, Franklin CC, Nair SS. Intrinsic mechanisms stabilize encoding and retrieval circuits differentially in a hippocampal network model. Hippocampus. 2014; 24:1430–1448. [PubMed: 24978936]

Izhikevich, EM. Dynamical systems in neuroscience: the geometry of excitability and bursting. London: MIT Press; 2010.

Johnson LR, Hou M, Prager EM, LeDoux JE. Regulation of the fear network by mediators of stress: norepinephrine alters the balance between cortical and subcortical afferent excitation of the lateral amygdala. Front Behav Neurosci. 2011; 5:23. [PubMed: 21647395]

Kim D, Paré D, Nair SS. Mechanisms contributing to the induction and storage of Pavlovian fear memories in the lateral amygdala. Learn Mem. 2013a; 20:421–430. [PubMed: 23864645]

Kim D, Paré D, Nair SS. Assignment of model amygdala neurons to the fear memory trace depends on competitive synaptic interactions. J Neurosci. 2013b; 33:14354–14358. [PubMed: 24005288]

Kim D, Samarth P, Feng F, Pare D, Nair S. Synaptic competition in the lateral amygdala and the stimulus specificity of conditioned fear: a biophysical modeling study. Brain Struct Funct. 2015:1–20. [PubMed: 24248427]

Krasne FB, Fanselow MS, Zelikowsky M. Design of a neurally plausible model of fear learning. Front Behav Neurosci. 2011; 5:41. [PubMed: 21845175]

LeDoux JE. Emotion circuits in the brain. Annu Rev Neurosci. 2000; 23:155–184. [PubMed: 10845062]

Li G, Nair SS, Quirk GJ. A biologically realistic network model of acquisition and extinction of conditioned fear associations in lateral amygdala neurons. J Neurophysiol. 2009; 101:1629–1646. [PubMed: 19036872]

Loretan K, Bissiere S, Luthi A. Dopaminergic modulation of spontaneous inhibitory network activity in the lateral amygdale. Neuropharmacology. 2004; 47:631–639. [PubMed: 15458834]

Maren S, Yap SA, Goosens KA. The amygdala is essential for the development of neuronal plasticity in the medial geniculate nucleus during auditory fear conditioning in rats. J Neurosci. 2001; 21:RC135. [PubMed: 11245704]

Moren, J.; Balkenius, C. A Computational Model of Emotional Learning in the Amygdale. In: Mayer, J.; Berthoz, A.; D, F.; HL, R.; SW, W., editors. From Animals to Animats. Cambridge, MA: MIT Press; 2000. p. 383-391.

Moustafa AA, Gilbertson MW, Orr SP, Herzallah MM, Servatius RJ, Myers CE. A model of amygdala-hippocampal-prefrontal interaction in fear conditioning and extinction in animals. Brain Cogn. 2013:81.

Pape HC, Paré D. Plastic synaptic networks of the amygdala for the acquisition, expression, and extinction of conditioned fear. Physiol Rev. 2010; 90:419–463. [PubMed: 20393190]

Quirk GJ, Armony JL, LeDoux JE. Fear conditioning enhances different temporal components of tone-evoked spike trains in auditory cortex and lateral amygdala. Neuron. 1997; 19:613–624. [PubMed: 9331352]

Quirk GJ, Repa C, LeDoux JE. Fear conditioning enhances short-latency auditory responses of lateral amygdala neurons: parallel recordings in the freely behaving rat. Neuron. 1995; 15:1029–1039. [PubMed: 7576647]

Repa JC, Muller J, Apergis J, Desrochers TM, Zhou Y, LeDoux JE. Two different lateral amygdala cell populations contribute to the initiation and storage of memory. Nat Neurosci. 2001; 4:724–731. [PubMed: 11426229]

Rumpel S, LeDoux J, Zador A, Malinow R. Postsynaptic receptor trafficking underlying a form of associative learning. Science. 2005; 308:83–88. [PubMed: 15746389]

Sah P, Faber ES, Lopez De Armentia M, Power J. The amygdaloid complex: anatomy and physiology. Physiol Rev. 2003; 83:803–834. [PubMed: 12843409]

Samson RD, Paré D. A spatially structured network of inhibitory and excitatory connections directs impulse traffic within the lateral amygdala. Neuroscience. 2006; 141:1599–1609. [PubMed: 16753264]

Shouval HZ, Bear MF, Cooper LN. A unified model of NMDA receptor-dependent bidirectional synaptic plasticity. Proc Natl Acad Sci USA. 2002; 99:10831–10836. [PubMed: 12136127]

Tovote P, Fadok JP, Luthi A. Neuronal circuits for fear and anxiety. Nat Rev Neurosci. 2015; 16:317–331. [PubMed: 25991441]

Tully K, Bolshkov VY. Emotional enhancement of memory: how norepinephrine enables synaptic plasticity. Mol Brain. 2001; 3(15):1–10.

Tuunanen J, Pitkanen A. Do seizures cause neuronal damage in rat amygdala kindling? Epilepsy Res. 2000; 39:171–176. [PubMed: 10759304]

Vlachos I, Herry C, Luthi A, Aertsen A, Kumar A. Context-dependent encoding of fear and extinction memories in a large-scale network model of the basal amygdala. PLoS Comput Biol. 2011; 7:e1001104. [PubMed: 21437238]

Woodruff AR, Sah P. Networks of parvalbumin-positive interneurons in the basolateral amygdala. J Neurosci. 2007; 27:553–563. [PubMed: 17234587]

Yiu AP, Mercaldo V, Yan C, Richards B, Rashid AJ, Hsiang HL, Pressey J, Mahadevan V, Tran MM, Kushner SA, Woodin MA, Frankland PW, Josselyn SA. Neurons are recruited to a memory trace based on relative neuronal excitability immediately before training. Neuron. 2014; 83:722–735. [PubMed: 25102562]

Highlights

- Mechanisms implementing cellular competition during fear memory formation are unknown
- A biophysical network model provided insights into the intrinsic and synaptic mechanisms
- Only PNs with access to input about the conditioned stimulus participated in the competition
- PNs receiving the least disynaptic inhibition and having NE and DA receptors won the competition
- The overall level of inhibition also controlled the size of the fear memory trace

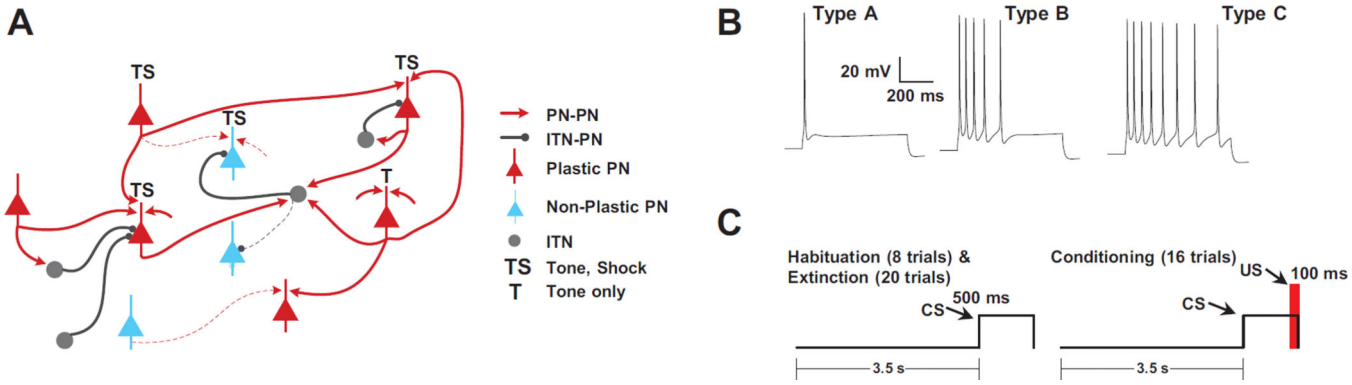

Figure 1.

Model structure, connections, and training protocol. ***A***. Cartoon of connectivity in the model that includes 800 PNs and 200 ITNs. Training induced changes to connections are indicated by solid lines, while connections that did not change are dotted. ***B***. Repetitive firing dynamics of three types (A, B, C) of model projection cells to 300 pA current injections. ***C***. Fear-conditioning protocol.

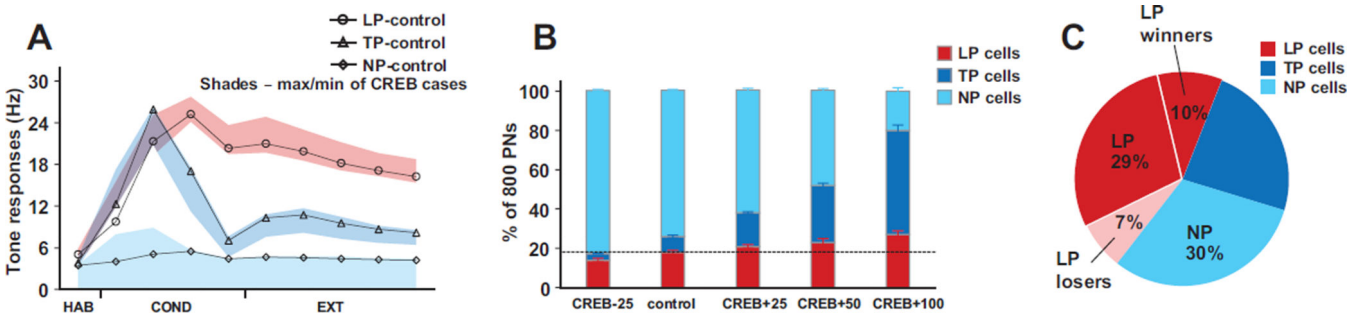

Figure 2.

Training-induced changes in output of model network. ***A***. Tone responses of LPs (circles), TPs (triangles) and NPs (diamonds) for the control case. Shaded areas around the control case denote the maximum and minimum of mean tone responses for the four CREB cases. All data points represent block of four trials, except for the first, which is the average of the final six habituation trials, as in Repa et al. (2001). ***B***. Changes in numbers of LPs (red), TPs (blue) and NPs (turquoise) across the four CREB cases. ***C***. Representative distribution of cell categories within the competition group (type B and C PNs that receive tone or tone and shock inputs). Also shows winner and loser numbers going from control to the $CREB^{+}25$ case. For panels C and D, the data were averaged across five different network instantiations of probabilistic connectivity gradients, for each case.

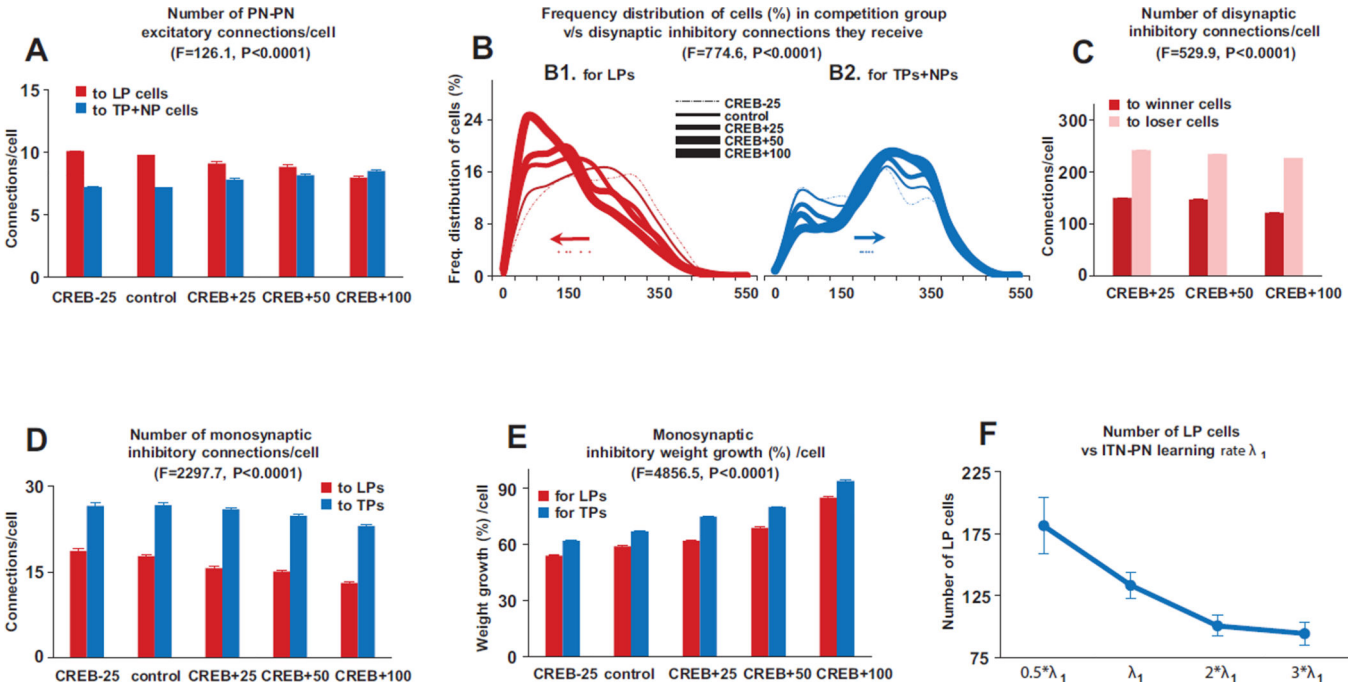

Figure 3.

Mechanisms that implement competition. The numbers in panels 2A and 2C were normalized to the control group case as follows: first the number of connections received by a cell was divided by the group size for the particular CREB case and then multiplied by the group size for the control case. ***A***. Within the competition group, LPs received significantly more monosynaptic excitatory inputs from other PNs than TP and NP cells for all the cases except the CREB^{+}100% condition (two way ANOVAs, F=126.1, DF=1, p<0.0001). ***B***. Frequency distribution of disynaptic inhibitory connections received by cells in the competition group for LPs (B1) and TPs+NPs (B2). The numbers have been normalized for the CREB cases by dividing by group size and then multiplying by the size of the control group. Dots represents the mean values of the disynaptic inhibitory connections for the various CREB cases, and the arrows points to the direction the mean moves with increasing CREB %s. LPs in the competition group received markedly less disynaptic inhibition from other competing PNs than TP and NP cells for all the cases (two way ANOVAs, F=774.6, DF=1, p<0.0001).***C***. The number of disynaptic inhibitory inputs from other PNs onto loser LPs, compared to those onto winner LPs, was significantly higher (two way ANOVAs, F=529.9, DF=1, p<0.0001). ***D***. Compared to LP cells, TP cells received considerably higher monosynaptic connections from ITNs across all CREB cases (Fig 2D; two way ANOVAs, F=2297.7, DF=1, p<0.0001). ***E***. Compared to LP cells, TP cells exhibited significantly higher growth in ITN-PN connections (Fig 2E; two way ANOVAs, F=4856.5, DF=1, p<0.0001). ***F***. Variation of LP cell numbers with changes in learning rate λ_1 for the ITN-PN connections. Data represent average ± SEM across five different network instantiations of probabilistic connectivity gradients for all panels except *F* which is over all the CREB cases.